Progress In Electromagnetics Research Letters, Vol. 96, 147–152, 2021

Frequency Reconfigurable Antenna with Conical Radiation Pattern and Wide Tuning Range

Jun-Yan Chen and Jeen-Sheen Row*

Abstract—The antenna is mainly composed of a suspended circular patch, eight shorting posts, and a ground plane. The circular patch is loaded with two concentric annular slots, and four varactors are placed across the outer annular slot to vary the resonant frequency of the antenna. Simulated results show that the resonant frequency can be tuned from 3.25 to 5.7 GHz as the capacitance of the varactors is varied from 0.2 to 12 pF, and conical radiation patterns are obtained when the antenna is operated at each resonant frequency. In the simulation, the reversed-bias circuit of the varactor is also included, and it is found that a bias tee or an inductor is not necessary for the proposed reconfigurable antenna. Experiments are also realized using two different varactors, and the measured results indicate that the peak gains of the conical radiation patterns occur around $\theta = \pm 40°$, and they are about 4.5 ± 1.5 dBi when the constructed prototypes are operated in the frequency range from 3.1 to 5.7 GHz.

1. INTRODUCTION

Frequency reconfigurable antennas have received much attention because they are helpful to increase spectrum utilization efficiency and relax the requirements of filters. A considerable number of designs related to the frequency reconfigurable antenna have been reported [1–12]. A linear slot antenna is often used to realize the frequency reconfigurable design, and the antenna operation band can be controlled with the PIN diodes embedded into the slot. A typical design is described in [2], and it can provide six discrete operation bands between 2.2 and 4.75 GHz; besides, the radiation pattern of the antenna at each band is bidirectional. The design in [3] is based on a shorted microstrip antenna resonant at the quarter-wavelength mode, and the resonant frequency can be tuned with PIN diodes connected to the non-radiating edges of the patch. The frequency tunable range of the antenna is from 2.35 to 3.43 GHz, leading to an available operation bandwidth of 37%, and broadside radiation patterns are obtained within the bandwidth. A bow-tie dipole is also adopted to design a frequency reconfigurable antenna [4], and its half-wavelength resonant frequency can be continuously tuned by placing PIN diodes and varactors into the dual radiating arms. The antenna achieves a tunable bandwidth of 51% with stable dipole–like radiation patterns. For traditional wireless communication systems, an antenna with vertically-polarized omnidirectional radiation is preferred, and a frequency reconfigurable antenna with θ-polarized conical radiation patterns is proposed in [5], where eight varactors are introduced into a monopolar patch antenna structure. The antenna is operated in TM_{01} mode, and the resonant frequency can be tuned from 1.64 to 2.12 GHz, forming an available operation bandwidth of 25%.

The purpose of this paper is to design a frequency reconfigurable conical-beam antenna with a wide tuning range. The design is based on a suspended patch antenna. The antenna can be operated in TM_{01}, TM_{02} [13], or wire-patch modes [14], and all of the modes can generate conical radiation patterns. In addition, the resonant frequency of each mode is related to the capacitance of the varactors embedded

Received 6 February 2021, Accepted 24 February 2021, Scheduled 1 March 2021
* Corresponding author: Jeen-Sheen Row (jsrow@cc.ncue.edu.tw).
The authors are with the Department of Electrical Engineering, National Changhua University of Education Chang-Hua, Taiwan 500, R.O.C.

into the patch. Consequently, the operation frequency of the proposed antenna has a wide tuning range of more than 50%, and stable radiation characteristics are also yielded across whole operation frequencies. The outline of this paper is as follows. The antenna structure and simulated results are presented in Section 2. Measured results are shown in Section 3. Finally, conclusions are given in Section 4.

2. ANTENNA STRUCTURE AND SIMULATED RESULTS

Figure 1(a) is the side view of a probe-fed suspended patch antenna. The top layer is a slotted patch fabricated on an FR4 substrate with thickness 0.8 mm and permittivity 4.4. The copper foil of the bottom FR4 substrate serves as the ground plane, and it is a square with a side length of 100 mm. The two FR4 substrates are separated with an air gap of 5 mm thickness, and the top substrate is supported by eight copper tubes shorted to the ground plane. The slotted patch is embedded with two concentric annular slots, and its detailed layout is presented in Fig. 1(b). Four SMD (surface mount device) capacitors ($C = 100$ pF) are placed across the inner annular slot, and four varactors are mounted across the outer annular slot. For varying the capacitance (C_V) of the varactors, a single-core sheathed conductor, passing through the inner hole of a copper tube, is used as a DC (direct current) line, and its one end is connected to the position close to the outer edge of the inner annular slot and the other end is directly linked to a power supply (V_0). The DC bias and RF (radio frequency) signal share the same ground plane. As for the SMD capacitors, they are introduced to prevent the DC bias from entering into the probe feed located at the center of the slotted patch. Note that the effects of the DC line on antenna performances are very few, and consequently a wideband bias tee is not necessary for the proposed reconfigurable antenna.

For the antenna with the parameters shown in Fig. 1, simulation analyses are performed with HFSS (High Frequency Structure Simulator). In the simulation, each varactor is modelled as a pure capacitor with capacitance C_V, and the effects of the DC line are included. Fig. 2(a) illustrates the return loss at the feed port for different cases of C_V, and it indicates that the antenna has good impedance matching for each studied case. The resonant frequency f_R, defined as the frequency with minimum return loss, is 5.7 GHz as C_V is 0.2 pF, and it is decreased to 3.25 GHz when C_V is increased to 12 pF. The variations of f_R against C_V are also presented in Fig. 2(b). It has to be mentioned that f_R can be further increased for the case of C_V lower than 0.2 pF; however, f_R is almost fixed for the case of C_V larger than 12 pF. To explore the resonant modes of the antenna operating at different frequencies, the distributions of the electric fields in the air gap are inspected, and the results for the cases of $C_V = 12$, 1, and 0.2 pF

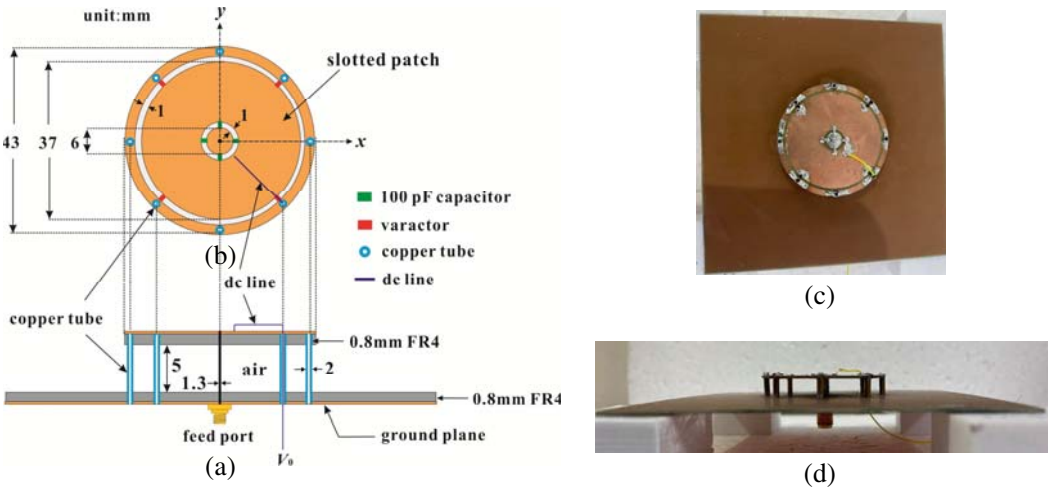

Figure 1. Geometry of the proposed antenna; the size of the ground plane is $100 \times 100\,\text{mm}^2$. (a) Side view of the antenna structure, (b) layout of the slotted patch, (c) top-view photograph of the constructed prototype, (d) side-view photograph of the constructed prototype.

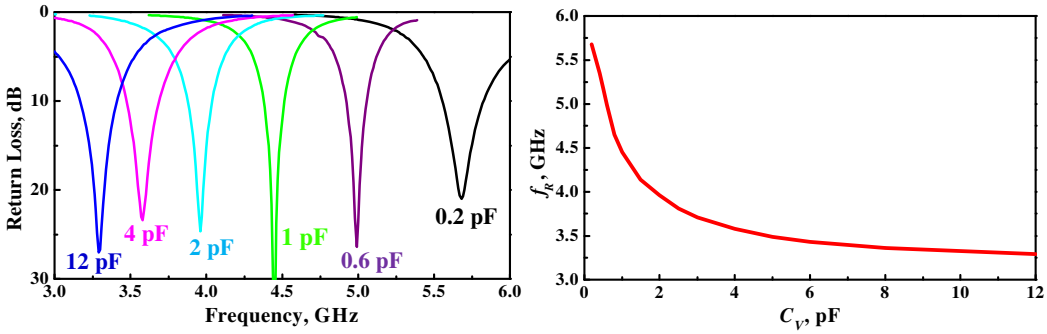

(a) (b)

Figure 2. Simulated results of the antenna with different C_V. (a) Return loss for the cases of $C_V = 0.2, 0.6, 1, 2, 4$, and 12 pF, (b) variations of f_R against C_V.

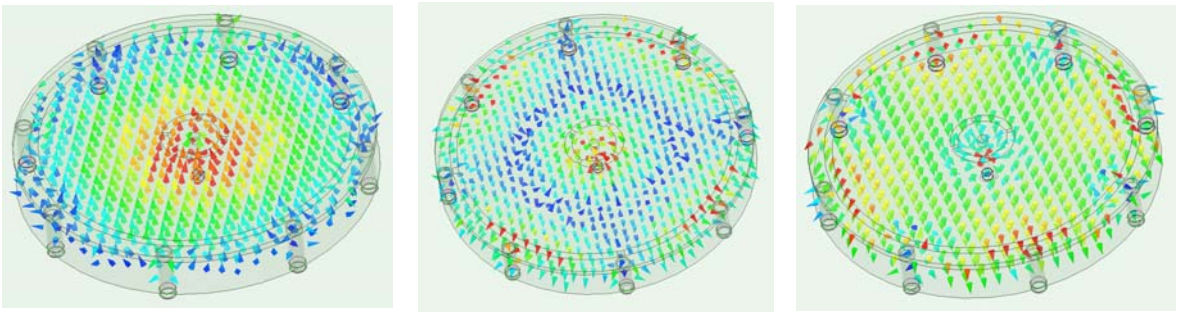

(a) (b) (c)

Figure 3. Distributions of electric fields in the air gap as the antenna resonant at various frequencies. (a) $f_R = 3.25$ GHz ($C_V = 12$ pF), (b) $f_R = 4.4$ GHz ($C_V = 1$ pF), (c) $f_R = 5.7$ GHz ($C_V = 0.2$ pF).

are exhibited in Figs. 3(a), 3(b), and 3(c), respectively. Observing Fig. 3(a), it is found that all of the electric fields have the same directions, and the antenna at 3.25 GHz is resonant at the TM_{01} mode; on the contrary, reverse electric fields are observed in Fig. 3(b), and the antenna at 4.4 GHz is operated in the TM_{02} mode [13]. As for Fig. 3(c), the maxima of the electric fields occur at the positions around the copper tubes, suggesting that the antenna at 5.7 GHz can be regarded as a monopole top-loaded with a shorted patch [14]. Note that the distributions of the electric fields would be obviously affected if an additional conducting wire appears in the air gap. That is why the DC line needs to be placed in the copper tube.

The simulated radiation patterns for the cases of $C_V = 12$, 1, and 0.2 pF are plotted in Figs. 4(a), 4(b), and 4(c), respectively. In addition to x-z ($\phi = 0°$) and y-z ($\phi = 90°$) planes, the radiation patterns in the plane ($\phi = -45°$) containing the DC line are also provided. These results clearly demonstrate that the antenna operating at different frequencies can give stable conical radiation patterns. The gain variations against frequency are shown in Fig. 5. The simulated peak gain at 3.25 GHz is about 3.8 dBi, and it is increased to 6.4 dBi at 5.7 GHz. As for the antenna efficiency, it is higher than 80% as the operation frequency ranges from 3.25 to 5.7 GHz.

3. MEASURED RESULTS

A prototype of the proposed antenna is constructed, and its photographs are exhibited in Figs. 1(c) and 1(d). Because the varactor which can entirely cover the capacitances from 0.2 to 12 pF is not available, we use two different varactors to validate the simulated results. One is BB857 diode from Infineon Technologies, and its capacitance can be varied from 0.5 to 7 pF. The other is MA46H120 diode from MACOM Technology Solutions, and its capacitance can range between 0.2 to 1.1 pF. First, four

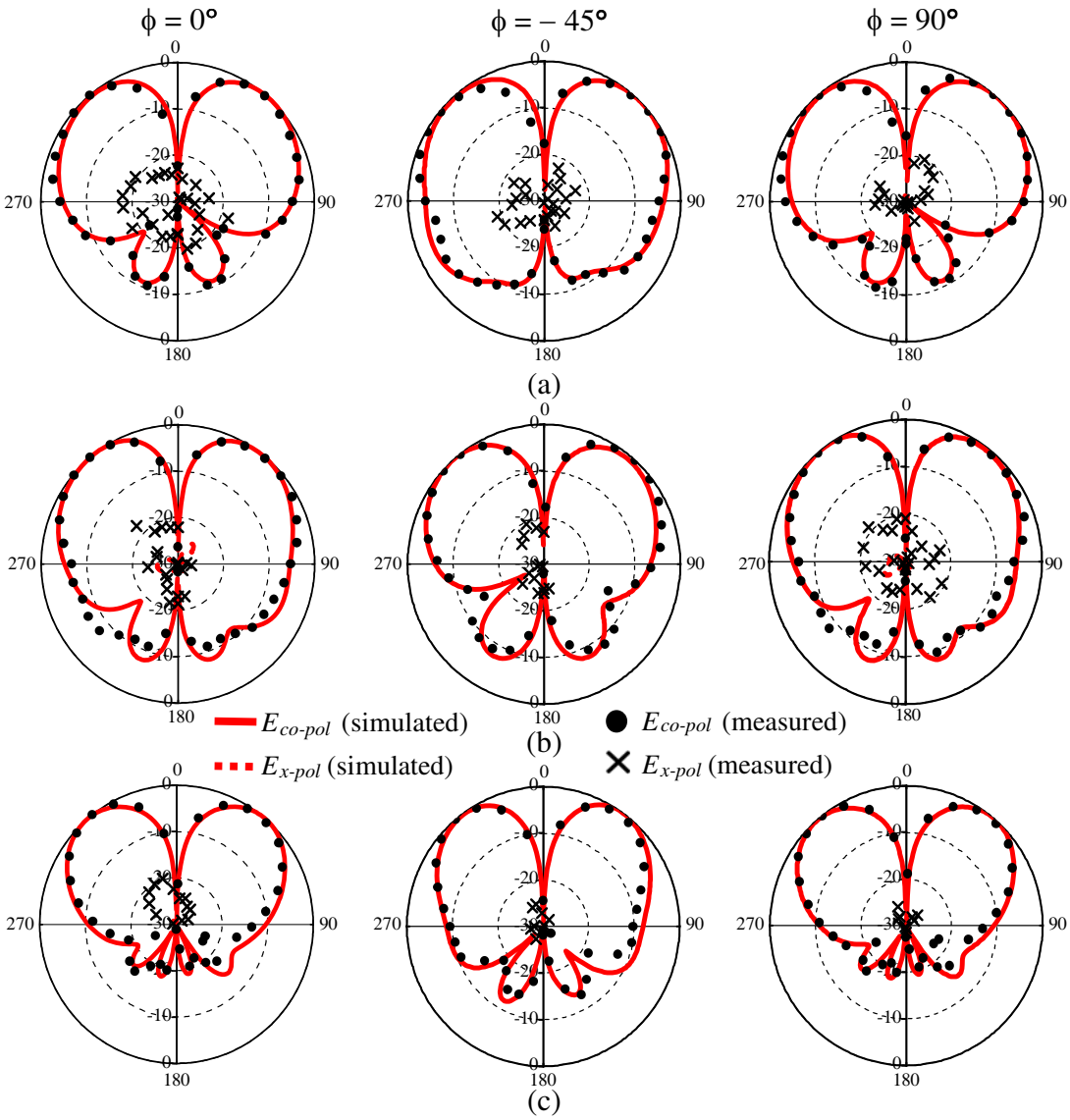

Figure 4. Simulated and measured radiation patterns in $\phi = 0°$, $-45°$, and $90°$ planes for the antenna operated at different frequencies. (a) 3.25 GHz ($C_V = 12$ pF), (b) 4.4 GHz ($C_V = 1$ pF), (c) 5.7 GHz ($C_V = 0.2$ pF).

of the BB857 diodes are mounted on the outer annular slot of the prototype, and the measured return loss is manifested in Fig. 6(a). From the results, it can be seen that, as V_0 is raised from 0 to 30 V, $\underline{f}_R$ is increased from 3.1 to 4.9 GHz, leading to a tunable range of 45%. Then, the MA46H120 diodes are introduced into the prototype instead of the BB857 diodes. The experimental results, shown in Fig. 6(b), demonstrate that $\underline{f}_R$ is moved from 4.1 to 5.7 GHz with increasing V_0, and a tunable range of 33% is obtained. The radiation patterns of the prototype are tested, and typical results are also plotted in Fig. 4 for comparisons. Measured and simulated results have good agreements, and both of them show that, for each frequency, the peak gain of the conical radiation pattern occurs around $\theta = \pm 40°$. The variations of measured peak gains against frequency are given in Fig. 5. As compared with the simulated data, the experimental gains are somewhat lower, and the errors mainly come from ohmic loss of the varactors. From Fig. 5, it is found that the loss of using the MA46H120 diode is smaller than that of using the BB857 diode, which proves the fact that the quality factor of the MA46H120 diode is obviously higher than that of the BB857 diode.

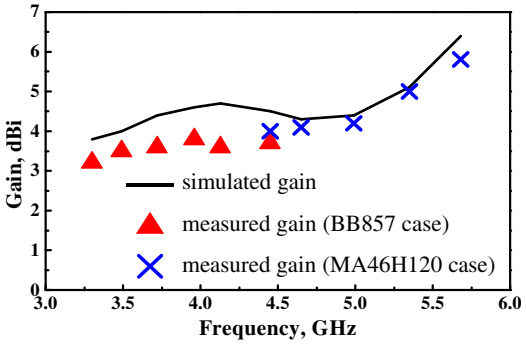

Figure 5. Variations of gains against frequency.

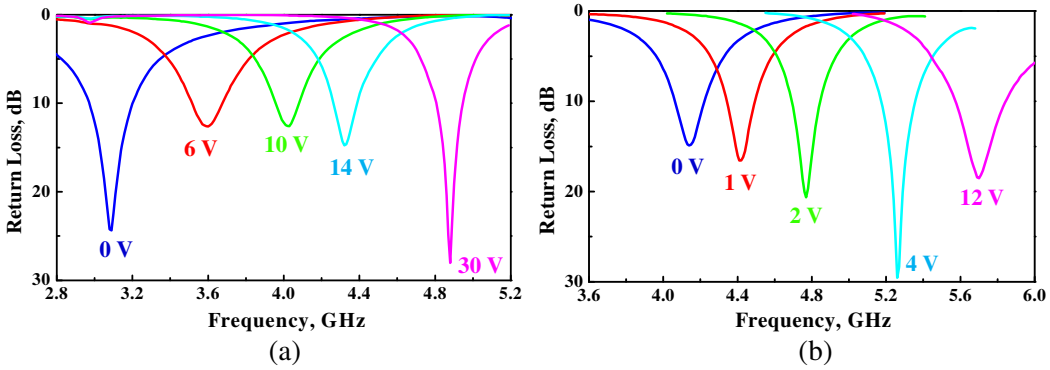

Figure 6. Measured return loss of the constructed prototype with various reverse biases V_0. (a) The case of using BB857 diodes, (b) the case of using MA46H120 diodes.

4. CONCLUSIONS

A design of frequency reconfigurable patch antennas has been presented. Three resonant modes can be well excited from the proposed antenna, and their resonant frequencies can be tuned with varactors embedded into the radiating patch. As a consequence, the operation frequency of the reconfigurable antenna has a wide tuning range. Moreover, all of the modes give conical radiation patterns, and stable radiation characteristics are obtained as the operation frequency is varied. Experiments has also been carried out, and the measured results have satisfactory agreements with simulated data. Because the two constructed prototypes are operated at the frequency bands from 3.1 to 4.9 GHz and from 4.1 to 5.7 GHz, they would be applied into UMB (ultra-wide band) and WLAN (wireless local network) systems, respectively. For practical applications, a smaller ground plane is preferred, and its effects on radiation characteristics will be studied in the future work.

REFERENCES

1. Shirazi, M., J. Huang, T. Li, and X. Gong, "A switchable-frequency slot-ring antenna element for designing a reconfigurable array," *IEEE Antennas Wireless Propag. Lett.*, Vol. 17, 229–233, 2018.
2. Majid, H. A., M. K. A. Rahim, M. R. Hamid, and M. F. Ismail, "A compact frequency-reconfigurable narrowband microstrip slot antenna," *IEEE Antennas Wireless Propag. Lett.*, Vol. 11, 616–619, 2012.
3. Boukarkar, A., X. Q. Lin, Y. Jiang, and X. F. Yang, "A compact frequency-reconfigurable 36-states patch antenna for wireless applications," *IEEE Antennas Wireless Propag. Lett.*, Vol. 17, 1349–1353, 2018.

4. Li, T., H. Zhai, L. Li, and C. Liang, "Frequency-reconfigurable bow-tie antenna with a wide tuning range," *IEEE Antennas Wireless Propag. Lett.*, Vol. 13, 1549–1552, 2014.
5. Ge, L. and K. M. Luk, "Frequency-reconfigurable low-profile circular monopolar patch antenna," *IEEE Trans. Antennas Propag.*, Vol. 62, 3443–3449, 2014.
6. Esmaeili, M. and J.-J. Laurin, "Polarization reconfigurable slot-fed cylindrical dielectric resonator antenna," *Progress In Electromagnetics Research*, Vol. 168, 61–71, 2020.
7. Singh, P. P., S. K. Sharma, and P. K. Goswami, "A compact frequency reconfigurable printed antenna for WLAN, WiMAX Multiple applications," *Progress In Electromagnetics Research C*, Vol. 106, 151–161, 2020.
8. Fertas, F., M. Challal, and K. Fertas, "A compact slot-antenna with tunable-frequency for WLAN, WiMAX, LTE, and X-Band applications," *Progress In Electromagnetics Research C*, Vol. 102, 203–212, 2020.
9. Hussain, R., M. S. Sharawi, and A. Shamim, "4-element concentric pentagonal slot-line-based ultra-wide tuning frequency reconfigurable MIMO antenna system," *IEEE Trans. Antennas Propag.*, Vol. 66, 4282–4287, 2018.
10. Nguyen-Trong, N., L. Hall, and C. Fumeaux, "A frequency- and pattern-reconfigurable center-shorted microstrip antenna," *IEEE Antennas Wireless Propag. Lett.*, Vol. 15, 1955–1958, 2016.
11. Ge, L., M. Li, J. Wang, and H. Gu, "Unidirectional dual-band stacked patch antenna with independent frequency reconfiguration," *IEEE Antennas Wireless Propag. Lett.*, Vol. 16, 113–116, 2017.
12. Chaouche, Y. B., F. Bouttout, M. Nedil, I. Messaoudene, and I. B. Mabrouk, "A frequency reconfigurable U-shaped antenna for dual-band WiMAX/WLAN systems," *Progress In Electromagnetics Research C*, Vol. 87, 63–71, 2018.
13. Liu, J., Q. Xue, H. Wong, H. W. Lai, and Y. Long, "Design and analysis of a low-profile and broadband microstrip monopolar patch antenna," *IEEE Trans. Antennas Propag.*, Vol. 61, 11–18, 2013.
14. Lin, S. J. and J. S. Row, "Monopolar patch antenna with dual-band and wide-band operations," *IEEE Trans. Antennas Propag.*, Vol. 56, 900–903, 2008.